

Citation for published version:

Argyle, IS, Wright, CJ & Bird, MR 2017, 'The effect of ethanol pre-treatment upon the mechanical, structural and surface modification of ultrafiltration membranes', *Separation Science and Technology*, vol. 52, no. 12, pp. 2040-2048. <https://doi.org/10.1080/01496395.2017.1310234>

DOI:

[10.1080/01496395.2017.1310234](https://doi.org/10.1080/01496395.2017.1310234)

Publication date:

2017

Document Version

Peer reviewed version

[Link to publication](#)

This is an Accepted Manuscript of an article published by Taylor & Francis in *Separation Science and Technology* on 28th March 2017, available online: <http://www.tandfonline.com/10.1080/01496395.2017.1310234>

University of Bath

General rights

Copyright and moral rights for the publications made accessible in the public portal are retained by the authors and/or other copyright owners and it is a condition of accessing publications that users recognise and abide by the legal requirements associated with these rights.

Take down policy

If you believe that this document breaches copyright please contact us providing details, and we will remove access to the work immediately and investigate your claim.

The effect of ethanol pre-treatment upon the mechanical, structural and surface modification of ultrafiltration membranes

Iain S. Argyle¹, Christopher J. Wright², Michael R. Bird^{1*}

¹Membrane Applications Laboratory, Department of Chemical Engineering,
University of Bath, BA2 7AY, UK

²College of Engineering, University of Swansea, Bay Campus, Fabian Way, Crymlyn Burrows,
Swansea, SA1 8EN, Wales, UK

*Corresponding author. Email: m.r.bird@bath.ac.uk

Abstract: The *in situ* ethanol pre-treatment of commercially available polysulfone (PSU) ultrafiltration (UF) membranes resulted in a 3-fold increase in the pure water flux (PWF) values achieved. Techniques that lead to an increase in flux are of both academic and commercial interest. It is postulated that the mechanisms for performance improvement can be attributed to swelling of membrane skin-layers, as demonstrated by changes in thickness measurements, and consideration of polymer solubility parameters, giving a degree of polymer plasticisation. The modification is accompanied by a hydrophobicity increase – this parameter is linked to a greater fouling tendency. Increases in hydrophobicity contrast with the usual effect of ethanol contact, by enhancing the removal of membrane preservatives and polyvinylpyrrolidone (PVP); a common pore-forming agent. Mechanical property changes were not readily detected, whilst the apparently unaltered sub-layer masked more subtle changes occurring within the dense skin-layer. Directing analysis specifically at the skin layer using colloidal AFM probes allowed a decoupling of changes against the support, showing that the elastic modulus was reduced as a consequence of PVP removal and plasticisation. Moreover, regional elasticity probing allowed observation of spatial inhomogeneities in elasticity; occurring due to the removal of the previously unevenly distributed PVP and leading to pitting. Consequently, the effects of pre-treatment with ethanol are shown to offer advantages by maximising the performance of commercial membranes, though such methods must be used with caution. Elasticity changes that occur may be detrimental to performance if carried out at high transmembrane pressures, where compaction could be assisted.

Highlights:

- *In situ* ethanol pre-treatment of polysulfone ultrafiltration membranes carried out
- Treatment resulted in a 3-fold increase in the pure water flux values achieved
- Performance improvement can be attributed to swelling of membrane skin-layers
- Elastic modulus reduced due to polyvinylpyrrolidone removal and plasticisation
- Despite flux increases, membrane life may be affected, and caution is needed

Keywords: ultrafiltration, pre-treatment, ethanol, fouling, cleaning.

1 Introduction

Membrane process performance is judged by both selectivity and permeability. Such performance is limited by a number of factors, though none more so than fouling. Strategies to alleviate the effects of fouling generally fall into four broad categories:

- Manipulating process variables to eliminate or minimise fouling. Factors such as refining the membrane material selection, the formulation and synthesis of membranes, mass transfer and fluid dynamic considerations (eg operating below the critical flux) and module design fall into this category.
- Feedstock pre-treatment. This area involves solute chemical adjustment (e.g. conductivity, pH, viscosity, temperature) to adjust solute solubility or affinity for membranes, as well as addition of insoluble particulates to aid filtration.
- Cleaning regime optimisation. Cleaning membranes in place as effectively as possible reduces process down time and chemical consumption. Membranes can also show synergistic responses following fouling and cleaning, acting to improve process performance cycle on cycle [1].
- Pre-treatment of membranes prior to operation. Whilst developing new membranes may take years and is an expensive process, modifying already existing commercial membranes can produce 'quick wins', resulting in a lower fouling tendency or an improvement in selectivity [2, 3].

In the context of this paper, pre-treatment of membranes is regarded as a post-synthesis step prior to filtration. Methods to pre-treat polymeric membranes in this context can be broadly classified as adsorptive treatments or coatings. Lohokare et al. [4] showed that polyacrylonitrile membranes could be modified by aqueous bases, both organic (ethanolamine/trimethylamine) and inorganic (NaOH, KOH). Permeation of water was enhanced for up to 12 hours for inorganic membrane treatments. However, treatment resulted in an eventual loss of permeability and deterioration in protein rejection performance. Ma et al. [5] showed that an immersive HCl treatment applied to polyvinyl butyral membranes hydrophilised the surface, and improved permeability. The authors attributed the mechanism of change to acid-catalysed hydrolysis of the polymer.

Treating UF membranes with alcohols or other organic solvents to modify their performance is an under-researched area. A study by Lencki and Williams [6] showed the effects of three non-aqueous solvents on PSU and regenerated cellulose membranes. Treatment with pure ethanol caused a 5-fold decrease in resistance compared to pure water for a 10 kDa PSU membrane, though contrastingly, a 30 kDa PSU membrane showed a 2-fold increase in resistance for the same conditions. The authors attributed the resistance variation recorded to various swelling mechanisms leading to constriction or expansion of pores. Transport processes were modelled using a semi-empirical approach based around a power-law

expansion of a common pressure-resistance relationship, and incorporating swelling parameters. However, the inherent variability of membrane configurations, even those consisting of the same base material, may reduce the usefulness of this modelling approach.

Kochan et al. [7] also showed that up to 3-fold increases in water fluxes occurred for polyethersulfone (PES) and PSU membranes tested in hollow fibres and flat sheet configurations. These substantial flux uplifts were also principally attributed to polymer swelling caused by solvents. Swelling parameters were used as the sole mechanistic explanation, after confirming these membranes showed no changes in wetting properties. This work offered an insight into how ethanol could perform as a treatment agent as opposed to the solute carrying solvent. However, the assumption that swelling is the sole mechanism of flux improvement requires further validation. It has been shown that ethanol modifies contact angles and the apparent zeta potential inside pores, resulting in substantial changes [1, 2]. Understanding why these changes occur is the key, along with a characterisation of the effect of swelling upon both the mechanical and structural properties of the membrane. Modification of chemical compositional changes is also reported.

2 Materials and Methods

2.1. Alcohol pre-treatment *in-situ*

All membranes were housed in an *Amicon*-type filtration cell (*Millipore*, USA) connected to a feed reservoir pressurised by nitrogen gas. UF membranes with a nMWCO of 50 kDa (GR51PP, *Alfa Laval*, Denmark) were first pre-conditioned by fluxing with hot reverse osmosis water under 1.0 bar TMP for 90 minutes, following an initial 10 minutes cycle under 4.0 bar TMP. The hot water conditioning protocol was demonstrated to be sufficient to remove the glycerol preservative by Weis & Bird [8]. Following measurement of PWF at 22 °C, 100% ethanol (ACS grade, Sigma Aldrich, Gillingham, UK) was permeated through the membrane *in situ* under 1.0 bar in dead-end mode before closure of the module permeate line. The membrane remained under 1.0 bar hydrostatic pressure immersed in ethanol for 24 hours prior to thorough rinsing and re-measurement of permeability. Fluxes at various TMPs were measured by taking mass readings on a balance interfaced with a PC directly via USB. Mass readings were recorded every 30 seconds and permeability was deduced from linear fit of TMP vs. flux (flux was calculated by dividing volume of permeate by the time step per unit membrane area (28.7 cm²). Each treatment protocol was employed on 3 separate membrane samples, with all membranes being sourced from the same production batch.

2.2. Surface and leachate analysis

Membrane wetting properties were measured on air-dried membrane coupons using an OCA 15 Pro 15 goniometer (*DataPhysics Instruments GMBH*, Germany). 1 µL of deionised water was placed on the sample and allowed to equilibrate. Contact angle was measured from both sides of droplet images as calculated using the Laplace model of the line extrapolated from the droplet profile. Measurements were

performed 5 times on each substrates from replicates of 3 experiments giving mean and standard deviation of $n = 15$ measurements.

Fourier transform infra-red (FTIR) spectroscopy was performed on membrane surfaces and membrane leachates using a Spectrum 100 (*Perkin-Elmer*, USA) spectrometer to qualitatively confirm chemical characteristics. For a given sample, 64 interferograms were recorded between 600 cm^{-1} and 4000 cm^{-1} wavenumber. For membrane surfaces, peak identification was performed in both Spectrum Express v.1.0 software (*Perkin-Elmer*, USA) and from relevant literature. For membrane leachate, peaks were identified using Spectrum Express software and compared to spectra of a pure PVP used as a reference standard (obtained from *Sigma Aldrich*, UK).

Membrane leachate was collected and prepared for FTIR analysis as follows. 100 mL of ethanol was fluxed through 5 pre-conditioned membranes statically under 1.0 bar of pressure in an *Amicon*-type stirred cell (*Millipore*, USA). Ethanol was collected and recycled 3 times before being evaporated in an incubator at $40\text{ }^{\circ}\text{C}$ overnight in a petri-dish containing a standard microscope slide. Background spectra for slides were used as a baseline before FTIR analysis of the leachate residue.

2.3. Swelling, pore characterisation and polymer dissolution

Membrane swelling was determined by measuring the thickness changes of membranes samples, both control and treated, using a digital micrometer. Pore size distribution was measured using a mercury intrusion porosimeter (Autopore IV, *Micromeritics Instrument Corp*, USA). Pre-cut strips of freeze-dried membrane were packed in 3 cm^3 penetrometers giving a total sample weight of between 0.5 and 0.6 g. The sample chamber was evacuated to $100\text{ }\mu\text{mHg}$ before low pressure mercury intrusion analysis (0.54 to 30 psia) and high pressure analysis (30 to 30,000 psia) with 20 seconds equilibration between increments. The pressure range used was sufficient to measure a range from $330\text{ }\mu\text{m}$ down to 6 nm (based on theoretical calculations using the Washburn equation).

Theoretical swelling/dissolution of polymers in given solvents is determined by use of Hansen solubility parameters. The smaller the difference in total cohesive energy density (by accounting for the relative contributions of dispersion (δ_D), polar (δ_P) and hydrogen-bonding (δ_H) forces) the higher the polymer solubility will be in the chosen solvent. The total solubility parameter (δ) is calculated as follows:

$$\delta^2 = \delta_D^2 + \delta_P^2 + \delta_H^2 \quad (1)$$

2.4. Mechanical testing

Macroscopic mechanical properties were tested on a universal testing machine (model 3369, *Instron*, USA) equipped with a 100 N load cell. Dumbbell shaped cut-outs of membranes were used with narrow section lengths of 30 mm and width 4 mm. Membrane thickness was dependant on treatment type; the mean measured thickness was thus used for calculations. Tensile strength was calculated from the load per cross-sectional area of membrane. Strain was calculated as a percentage of the extension to the original length of the sample using a 1 mms^{-1} extension rate. Ultimate tensile strength was taken as the

maximum tensile strength before breakage. The corresponding strain to this point was termed the strain at break.

Surface elasticity measurements were performed using an atomic force microscope (AFM) (*Nanowizard 3*, JPK GMBH, Germany). A spherical silica colloidal probe (ca. 8.5 μm diameter) attached to a tipless cantilever (UL-CT-NT, Veeco, USA) using a UV-cured epoxy based glue. Cantilever calibration and blank probe interactions were characterised in 0.1 M NaCl buffer at pH 4.5 against a mica substrate. By subtraction of the deflection (calculated by deformation of the cantilever using Hooke's law) from the total distance moved by the piezo motor in the vertical (z) direction, the degree of indentation was calculated. Using the Hertz model rearranged for the elastic modulus, considering a parabolic tip (hemisphere) to calculate projected contact area, and assuming an isotropic and linearly elastic collision of probe to sample (Poisson's ratio of 0.5), elastic modulus was calculated (see equation 2):

$$F = \frac{4\sqrt{r_c}}{3} \frac{E}{1-\nu} s^{3/2} \quad (2)$$

Where F is the total force, r_c is the probe radius, E is the modulus of elasticity, ν is Poisson's ratio, and s is the degree of probe indentation. Measurements were taken in grids of 3 x 3 points in 9 separate locations (also arranged in a grid) over a 10 x 10 μm area of membrane.

3. Results and Discussion

3.1. Flux uplift and wetting modification

Following alcohol treatment with 100% ethanol, PWF had increased by a factor of three over pre-conditioned untreated membranes. This increase in flux also correlates positively with membrane hydrophobicity, a change from $74^\circ \pm 2^\circ$ to $85^\circ \pm 1^\circ$. The lower wettability of the membrane provides some evidence as to why the flux increases; through a rise in slip given the lower adhesion of water molecules directly adjacent to the pore walls. This assumes that any modification occurring on the surface also occurs inside the pores. Argyle et al. [9] showed that the through-pore negative zeta potential decreased upon ethanol treatment of PSU membranes. This indicated that the effect may arise due to a thin film of alcohol remaining on pore walls, resulting in a shielding of the true pore surface charge and consequently a reduction in the streaming potential value.

Water slip increase is the usual explanation given for the order of magnitude increase seen in flow through carbon nanotubes compared to that theoretically predicted by Poiseuille flow [10, 11]. The contact angles measured for these membranes are highly comparable to those systems reviewed by Mattia and Gogotsi [12] and thus give a firm indicator that the degree of water interaction with the surface may also be comparable. Whilst electrochemical effects influence wettability and result in lower energy surfaces, a more multi-faceted explanation is required to explain the changes seen in membrane performance.

Table 1: Pure water flux during treatment shows a near 3-fold increase over the untreated membrane. A higher static contact angle indicates a lower affinity for water. Errors are standard deviations calculated from $n = 3$ for permeability readings and $n = 15$ for contact angle measurements.

<u>Treatment type</u>	<u>Permeability/ $\text{Lm}^{-2}\text{hr}^{-1}\text{bar}^{-1}$</u>	<u>Static contact angle/$^{\circ}$</u>
Control (no treatment)	111 ± 6	74 ± 2
100% ethanol treatment	323 ± 12	85 ± 1

3.2. Surface and leachate chemical analysis

Chemical characterisation of membrane surfaces was performed using FTIR. It is unlikely that any modification to PSU would occur due to impurity reaction in the presence of ethanol as a solvent; nevertheless spectra obtained did display some subtle differences. A comparison of the membrane surface spectra shown in Figure 1a reveals a disappearance of spectral bands at 920 cm^{-1} and 1040 cm^{-1} . In addition, a weakening of the band at 2900 cm^{-1} was evident for treated membranes. Belfer et al. [13] showed that when conducting water/ethanol exchanges on PES membranes, losses in these specific bands could be attributed to the enhanced removal of preservatives. No indication of the specific preservatives was mentioned.

Weis et al. [8] stated that a peak at 1040 cm^{-1} for a pristine PSU membrane surface spectrum was indicative of an aliphatic alcohol, probably glycerol. Later, these authors introduced the use of $60 \text{ }^{\circ}\text{C}$ hot water pre-conditioning as means to reduce the viscosity of preservatives, and remove them from the membranes prior to usage [14]. Employing the same strategy as a pre-conditioning stage in this study (and further with ethanol treatment), clearly shows that additional alcohol treatment yields an enhanced removal of this peak, and thus a more effective removal of glycerol. In this latter study, the authors also stated that a masking of the band 1667 cm^{-1} was a result of membrane fouling. Membrane spectra here show that this band is present for the control, but that it is also revealed to a greater degree following ethanol treatment. Therefore the shielding of this peak may well be a result of the applied preservatives, and not as a result of fouling.

Analysis of the dried leachate (a translucent white gel-like layer) and comparison to a chemical library revealed an identical spectrum to that of PVP. Producing a spectrum from a sample of this material showed the near identical resemblance in peak occurrence (Figure 1b). Since PVP is readily soluble in water (hence its use as a pore forming/swelling agent in membrane fabrication), it would be expected that it would gradually be removed over time, and this removal could be enhanced through use of cleaning-in-place agents commonly used on such membranes e.g. alkalis, acids, hypochlorite and proprietary cleaning agents, as was suggested by Lindau et al. [15]. Observation of the Hansen solubility parameters (as commonly used for optimisation of solvent-polymer systems) for PVP in ethanol shows that the relative distance in the so-called Hansen Space is a factor of 5 closer for ethanol over water ($28.7 \text{ MPa}^{1/2}$ compared to $5.6 \text{ MPa}^{1/2}$) as calculated from equation 1 using data from [16]. This calculation confirms the superior solvency power of ethanol for PVP over water, and thus its ability to intensify removal from the porous network. This provides another fundamental explanation for the PWF performance increase, as well as enhanced removal of a hydrophilic agent from an otherwise quite moderately hydrophilic PSU membrane.

The inclusion of PVP in membrane casting formulations, which some authors have shown can alter the transmission of some key solutes [17, 18], gives a more hydrophilic membrane, as demonstrated here, and also reported by other workers [19]. There is also an associated increase in membrane surface zeta potential as determined through steaming current measurement made tangentially to the surface [20].

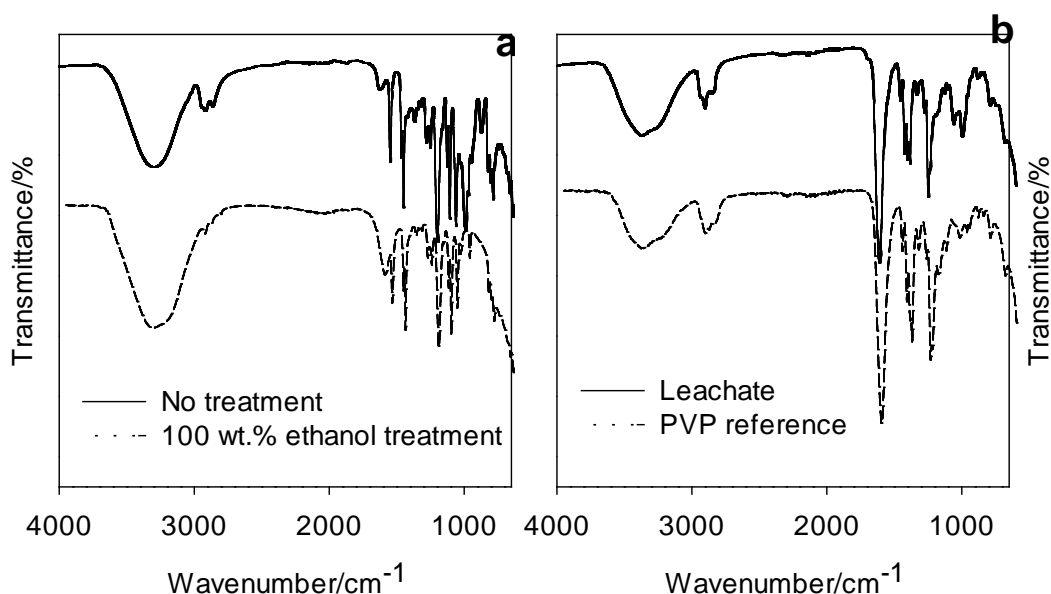


Figure 1: (a) Membrane surfaces exhibit subtle differences in surface chemistry following ethanol treatment as determined by FTIR spectra. (b) Membrane leachate is confirmed to be PVP showing that ethanol pre-treatment acts to remove this common pore forming agent.

3.3. Swelling and pore size distribution

Sample thickness measurement (Figure 2a) gives an indication that there is a macroscopic expansion of the membrane; the mean value of $n = 45$ measurements (15 from each membrane section) showing an increased from $140 \mu\text{m}$ to $156 \mu\text{m}$. Employing the unpaired two-tailed Student's t-test under the null hypothesis that there was no change in thickness relating to alcohol treatment returned a value of ≤ 0.01 i.e. a 99% certainty that the null hypothesis can be rejected.

To confirm that the active layer was swelling, the membrane support layer was isolated from the top layer by dissolution in a suitable solvent before drying and immersion in water or 100% ethanol. Respective thickness of this supports were $193 \pm 12 \mu\text{m}$ and $194 \pm 11 \mu\text{m}$ (global average being $193 \pm 11 \mu\text{m}$) and confirmed that the polypropylene support was not susceptible to swelling. Membranes following ethanol treatment also showed some flattening and relaxation (they are normally stored in rolls, and thus their natural shape is curved with the top layer on the concave side). Differential swelling of layers of composite membranes such as these has been shown to lead to deformation [21, 22]. Heffernan et al. [21] demonstrated that a polymeric nanofiltration membrane (polyamide supported on PSU, which was supported on polyester) showed similar relaxation behaviour to the samples examined here. It was demonstrated that the polyamide top layer had swelled to a greater degree than the PS. The result of the flattening seen in this study also reinforces the hypothesis that the one-dimensional swelling measured also acts principally in the lateral direction, although this expansion is likely to be restricted by the attachment of the active layer to the support substrate.

Figure 2b indicates that for pore sizes above 5×10^4 nm there is little difference between the control and ethanol treated systems. These sized pores are not deemed to be the active layer pores, and confirm that the propylene support does not show any significant modification in pore structure following treatment.

There is some slight deviation in the pore volumes in the lower pore diameter range. The peak size increase at 200 nm is significant. Differences between the treated and control membranes between 10 and 15 nm indicate an expansion in the pore size, and the number, following treatment. Confirmation as to whether swelling and expansion of the pore volume has been detected, and whether the stripping away of PVP inside the porous matrix has effectively increased the pore volume, or whether this is simply a result of changing materials properties remains unproven, and requires further investigation from complimentary techniques.

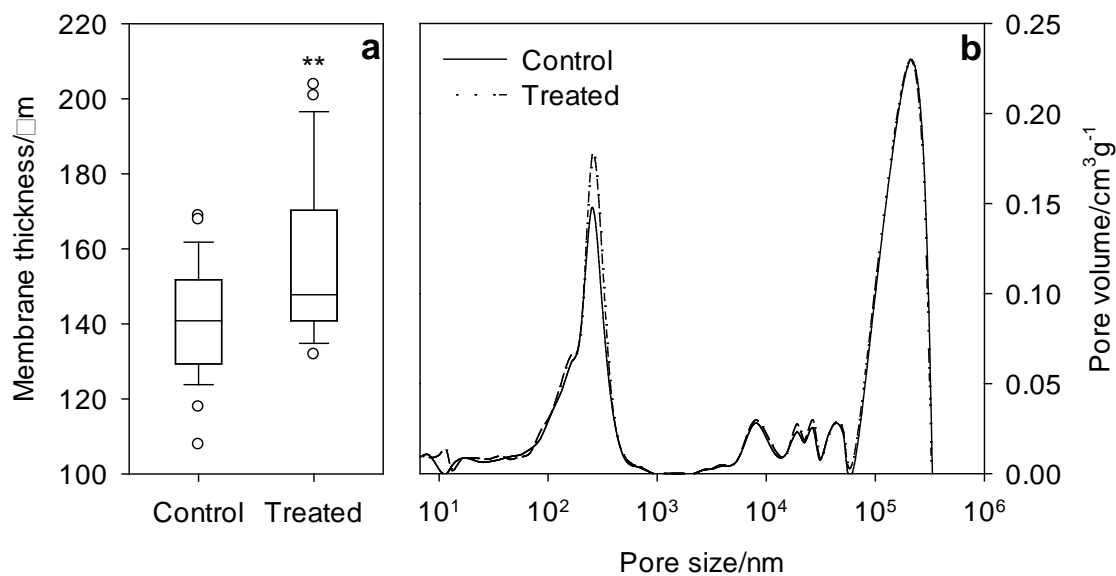


Figure 2: (a) PSU membrane shows macroscopic expansion after ethanol treatment as measured by membrane thickness. ** represents $P \leq 0.01$ for $n = 45$ measurements (193 ± 11 μm polypropylene support layer thickness has been subtracted). (b) Pore volume for a given pore size shows little change for large pores ($>10^4$ nm) indicating expansion of the membrane support layer does not occur. For smaller pores, some differences are apparent offering two potential theories; that either small pores in the membrane active layer are expanded upon treatment, or that elasticity modifications (shown in following section) can influence mercury intrusion porosimetry distribution profiles.

3.4. Macroscopic tensile properties

Assessing the macroscopic mechanical properties of materials is a useful means of testing potential for a given application, but also to assess whether treatments have caused any detrimental effects.

Typically, the ultimate tensile strength and elongation (or strain) at break are useful determined. If the material has a low proportionality and elastic limits, and deformation occurs at relatively low stresses, this is a particularly useful measure. Measurements shown here demonstrate that no significant change has occurred either in the ultimate tensile strength of the membrane, or the strain at break point as a result of ethanol treatment (see Figures 3a and 3b). The strain range over which the true elastic limit can be calculated is also small, and the curves are characterised by a long yield section before breakage. Given the already firm evidence that no changes occur to the support layer, and considering that the presence of this layer is indeed to provide mechanical support, these tests do not give a convincing indication of how the membrane modifications impact the mechanical properties, and hence the filtration capabilities of the membranes. Decoupling of a polyester support from PSU/polyamide has shown that individual layer tensile properties can be differ significantly from that of the composite material, and highlights the importance of being able to focus this type of analysis on the active layer (or layer of most interest) [21]. For the membranes in this study, decoupling the polypropylene support by peeling it away would have resulted in damage, and inconsistencies in sample preparation. Membrane preparation consists of casting one layer onto the other, and thus the membrane exhibits a form of self-adhesion during manufacture. An AFM was therefore used in an attempt to decouple and resolve any suspected mechanical variations, in addition to the differences shown by the other analytical methods.

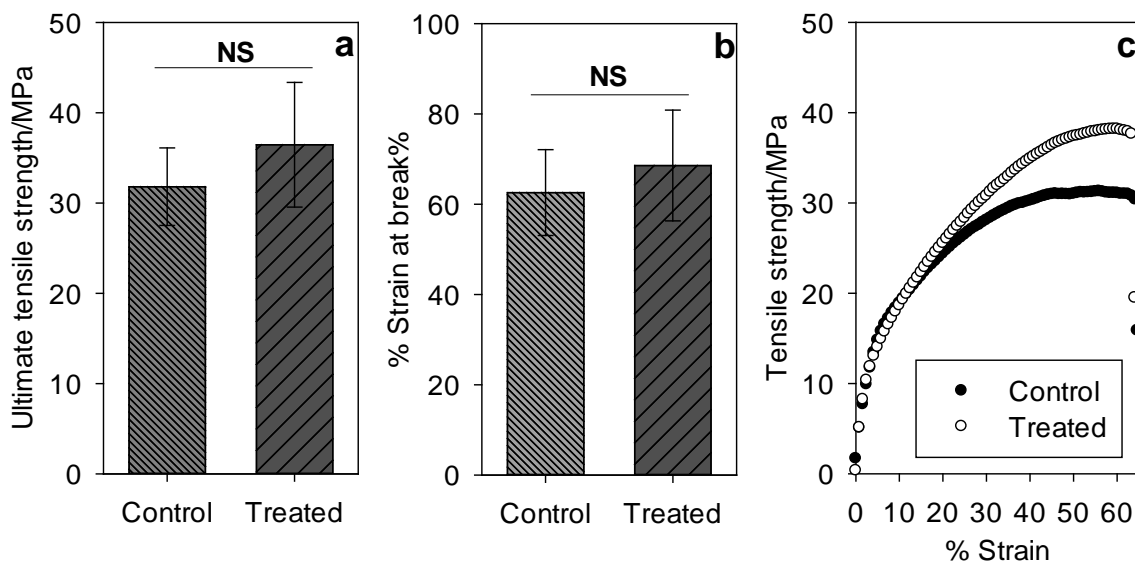


Figure 3: (a) Ultimate tensile strength, (b) Strain at break, and (c) Representative stress-strain curves for control and treated samples. Definition between tensile properties of membranes is difficult to resolve given the presence of the membrane backing layer. Whilst ductility is slightly increased for treated membranes, there is no statistical significance (NS) between data sets ($n = 16$).

3.5. Microscopic elasticity modification

Figure 4a shows the principle of elasticity measurement determination. There is a difference between the total z-displacement as the cantilever moves towards the surface, and the deflection experienced;

the difference is accountable by noting there is an indentation of the probe into the surface. The calculated elastic moduli show significantly different values for control and treated membranes (see Figure 4b). Figures 4c and 4d shows the result of scanning a given area of membrane with a colloidal probe attached to an atomic force microscope cantilever. The results are in stark contrast to the bulk properties shown in Figure 3. The values are all characteristic of what would be expected of a range of different polymers, though it is suspected that expansion of the porous substructure, removal of PVP from inside the membrane, and plasticisation of PSU would increase the surface elastic properties.

The spatial variation is characteristic of a softening of the material given the drop in elastic modulus. The rigidity of the polymer is lost in favour of a spongier surface. Whilst the AFM measurements revealed relative consistency on the untreated membrane, there is a more significant variation following treatment; some areas exhibiting elastic moduli of around 0.5 GPa. The variability is a significant point to note and can be related to maldistribution of PVP during membrane casting. This effect was shown by Koga et al. [23]. The authors showed that while a blanket scan using standard attenuated total reflectance FTIR showed consistency on the bulk surface of a PSU dialysis membrane, near-field IR revealed inhomogeneity in the distribution of PVP, with different areas exhibiting between 5% and 40% PVP content to PSU. If PVP is washed from both areas of high and low concentration by ethanol, then one would expect that the underlying foundation resisting the downward force of the AFM probe would also vary, and what the results show is a form of sub-surface pitting. The consistently lower elastic moduli for the treated surface would seem to suggest that the whole structure is indeed softening, though this could be attributed to both a decrease in the overall bulk density (expansion of the matrix) or partial dissolution of the polymer. If the Hansen solubility parameters are once again considered, the relative difference of ethanol to PSU is less than that of water and is predominantly due to the increased dispersive forces in the PSU-ethanol system.

When encountering a higher pressure operation, a softer and spongier porous network would likely lead to compaction and thus constriction of the membrane. Higher water post-treatment water fluxes gained could well turn into a negative effect, when the membrane is in normal usage.

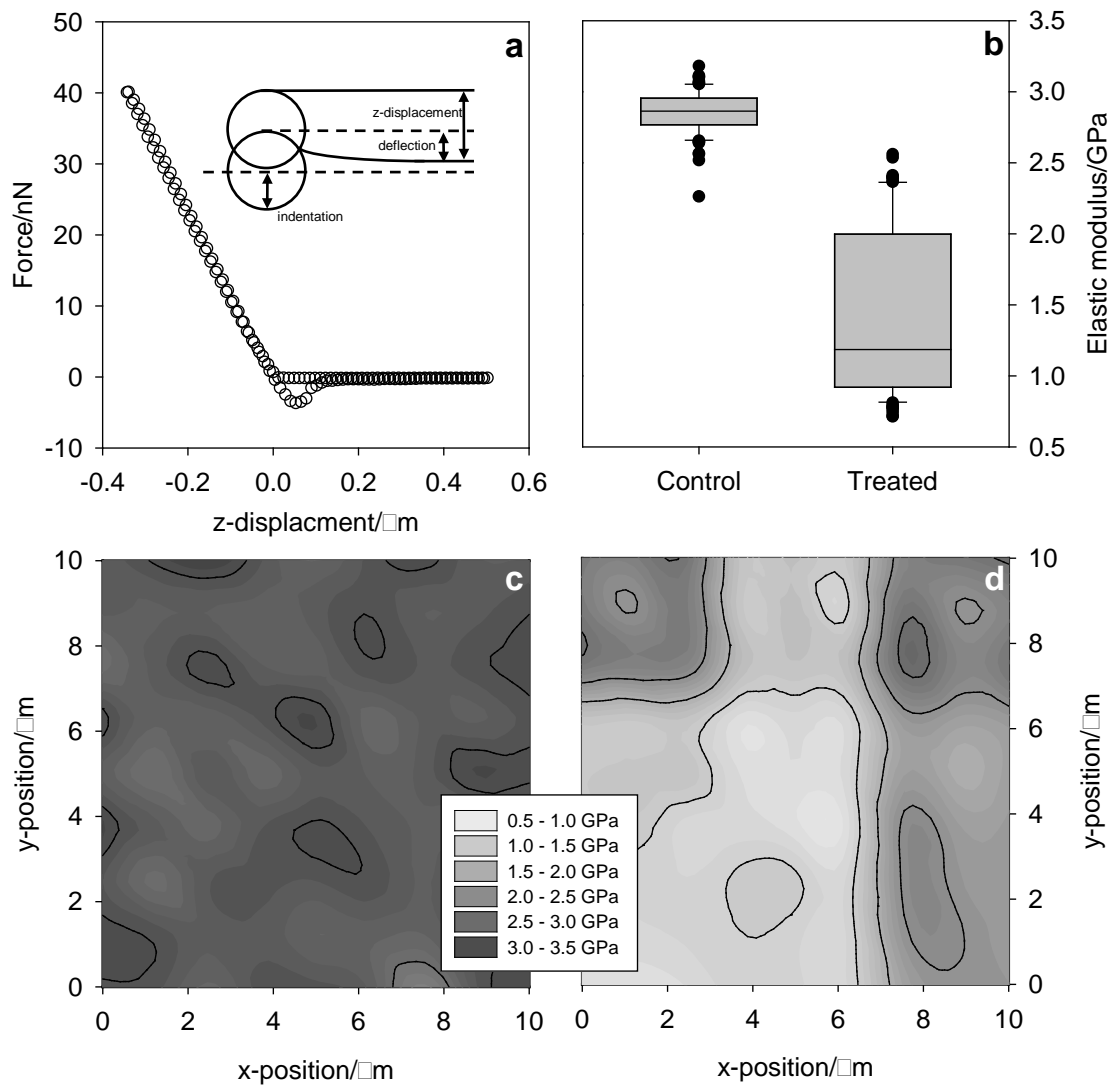


Figure 4: (a) representative AFM force curve and inset schematic showing the principal of measuring elasticity and (b) box plot indicating the difference in global elasticity measurements. Measurements over membrane surfaces reveal that control membrane (c) has a modulus of elasticity consistently in the range 2 – 3.5 GPa whereas the treated membrane (d) shows significant spatial inhomogeneity with the 10 × 10 μm sample area; the modulus of elasticity decreases to values lower that 1.0 GPa in some regions and is consistently below 2.5 GPa over the entire analysis area.

4 Conclusions and recommendations

It has been shown that an apparently simple ethanol pre-treatment method employed to increase the performance of a common industrial UF membrane can have far reaching-impacts upon the membrane water flux and surface chemical properties. This has been shown to be due to a multitude of factors, such as removal of PVP, which can alter both the hydrophilicity and porosity of the membrane, as well as the partial dissolution/swelling of the membrane based material. The typical mechanical tests employed to assess the condition of membranes have been insufficient to assess the true state of the membrane. However, it has been demonstrated that AFM mechanical measurements with relatively

large silica colloidal probes can successfully give microscopic resolution of surface mechanical properties. The results shown by this methodology indicate the factors contributing to the understanding of PSU membrane pre-treatment with ethanol, demonstrating that the removal of poorly dispersed PVP can produce a highly variable surface. Thus a key conclusion is that pre-fluxing with ethanol (for example to sterilise membranes, or filtrations in which ethanol is part or all of the feed solvent, such as in brewing or wine processing) should be attempted with caution. Whilst leading to an initial flux increase, the effect of initial and continued ethanol treatments may impact adversely upon the performance and lifetime of the membrane over multiple cycles.

Acknowledgements

The authors would like to thank Dr. Lydia Powell for assistance with AFM measurements and Dr. Frank Lipnizki of *Alfa Laval*, Denmark for supply of the membranes used in the study.

Funding Sources

This project was supported an Engineering and Physical Sciences Research Council (EPSRC) Doctoral Training Award.

Nomenclature

Symbol	Definition	SI Unit
E	Modulus of elasticity	Pa
F	Force	N
r_c	Radius of curvature	m
s	Indentation	m
ν	Poisson's ratio	-
δ	Cohesive energy density	Pa ^{0.5}

Subscripts:

D	Dispersion forces
H	Hydrogen bonds
P	Polar forces

References

1. Argyle, I.S., A. Pihlajamäki, and M.R. Bird (2015), 'Black tea liquor ultrafiltration: Effect of ethanol pre-treatment upon fouling and cleaning characteristics'. *Food and Bioproducts Processing*, **93**, pp. 289-297.
2. Argyle, I.S., A. Pihlajamäki, and M.R. Bird (2014), 'Ultrafiltration of black tea using diafiltration to recover valuable components'. *Desalination and Water Treatment*, **53(6)**, pp. 1532-1546.
3. Jones, S.A., M.R. Bird, and A. Pihlajamäki (2011), 'An experimental investigation into the pre-treatment of synthetic membranes using sodium hydroxide solutions'. *Journal of Food Engineering*, **105(1)**, pp. 128-137.
4. Lohokare, H.R, Kumbharkar, S.C., Bhole, S, and Kharul, U. K., (2006), 'Surface modification of polyacrylonitrile based ultrafiltration membrane'. *Journal of Applied Polymer Science*, **101(6)**, pp. 4378-4385.
5. Ma, X., Sun, Q., Su, Y., and Jiang, Z, (2007), 'Antifouling property improvement of poly (vinyl butyral) ultrafiltration membranes through acid treatment'. *Separation and Purification Technology*, **54(2)**, pp. 220-226.
6. Lencki, R.W. and S. Williams (1995), *Effect of nonaqueous solvents on the flux behavior of ultrafiltration membranes*. *Journal of Membrane Science*, **101(1-2)**, pp. 43-51.
7. Kochan, J., Wintgens, T., Hochstrat, R., and Melin, T., (2009), 'Impact of wetting agents on the filtration performance of polymeric ultrafiltration membranes'. *Desalination*, **241(1-3)**, pp. 34-42.
8. Weis, A., M.R. Bird, and M. Nyström (2003), The chemical cleaning of polymeric UF membranes fouled with spent sulphite liquor over multiple operational cycles. *Journal of Membrane Science*, **216(1-2)**, pp. 67-79.
9. Argyle, I.S., Bird, MR, 2014, 'Microfiltration of high concentration black tea streams for haze removal using polymeric membranes', *Desalination & Water Treatment*, **53, 6**, 1516-1531.
10. Holt, J.K., Park, H.G., Wang, Y., Stadermann, M., Artyukhin, A.B., Grigoropoulos, C.P., Noy A., and Bakajin, O., (2006), 'Fast mass transport through sub-2-nanometer carbon nanotubes'. *Science*, **312(5776)**, pp. 1034-1037.
11. Majumder, M., N. Chopra, and B.J. Hinds (2011), 'Mass transport through carbon nanotube membranes in three different regimes: Ionic diffusion and gas and liquid flow'. *ACS nano*, **5(5)**, pp. 3867-3877.
12. Mattia, D. and Y. Gogotsi (2008), 'Review: static and dynamic behavior of liquids inside carbon nanotubes'. *Microfluidics and Nanofluidics*, **5(3)**, pp. 289-305.
13. Belfer, S; Fainctain, R; Purinson, Y; Kedem, O., (2000) 'Surface characterization by FTIR-ATR spectroscopy of polyethersulfone membranes-unmodified, modified and protein fouled'. *Journal of Membrane Science*, **172(1)**, pp. 113-124.
14. Weis, A., et al. (2005), 'The influence of morphology, hydrophobicity and charge upon the long-term performance of ultrafiltration membranes fouled with spent sulphite liquor'. *Desalination*, **175(1)**, pp. 73-85.

15. Lindau, J., A. Jönsson, and A. Bottino (1998), 'Flux reduction of ultrafiltration membranes with different cut-off due to adsorption of a low-molecular-weight hydrophobic solute-correlation between flux decline and pore size'. *Journal of Membrane Science*, **149**(1), pp. 11-20.
16. Barton, A.F. (1991), *CRC handbook of solubility parameters and other cohesion parameters*: CRC press.
17. Susanto, H., Y. Feng, and M. Ulbricht (2009), Fouling behavior of aqueous solutions of polyphenolic compounds during ultrafiltration. *Journal of Food Engineering*, **91**(2), pp. 333-340.
18. Ulbricht, M., Ansorge, W., Danielzik, I and Schuster, O., (2009), 'Fouling in microfiltration of wine: The influence of the membrane polymer on adsorption of polyphenols and polysaccharides'. *Separation and Purification Technology*, **68**(3), pp. 335-342.
19. Marchese, J., Ponce, M., Ochoa, N.A., Prádanos, P., Palacio, L., and Hernández A.,. (2003), 'Fouling behaviour of polyethersulfone UF membranes made with different PVP'. *Journal of Membrane Science*, **211**(1), pp. 1-11.
20. Susanto, H. and M. Ulbricht (2009), Characteristics, performance and stability of polyethersulfone ultrafiltration membranes prepared by phase separation method using different macromolecular additives. *Journal of Membrane Science*, **327**(1), pp. 125-135.
21. Heffernan, R., Semiao, A.J.C., Desmond, P., Cao, H., Safari, A., Habimana, O. and Casey, E., (2013), Disinfection of a polyamide nanofiltration membrane using ethanol. *Journal of Membrane Science*, **448**, pp. 170-179.
22. Yang, X., Livingston, A., and Freitas dos Santos, L., (2001), Experimental observations of nanofiltration with organic solvents. *Journal of Membrane Science*, **190**(1), pp. 45-55.
23. Koga, S., Yakushiji, T., Matsuda, M., Yamamoto, K. and Sakai, K., (2010), Functional-group analysis of polyvinylpyrrolidone on the inner surface of hollow-fiber dialysis membranes, by near-field infrared microspectroscopy. *Journal of Membrane Science*, **355**(1), pp. 208-213.